Influence of Tertiary Structure Domain Properties on the Functionality of Apolipoprotein A-I[†]

Masafumi Tanaka,[‡] Mao Koyama,[‡] Padmaja Dhanasekaran,[§] David Nguyen,[§] Margaret Nickel,[§] Sissel Lund-Katz,[§] Hiroyuki Saito,[‡] and Michael C. Phillips*[,§]

Department of Biophysical Chemistry, Kobe Pharmaceutical University, Kobe 658-8558, Japan, and Lipid Research Group, Children's Hospital of Philadelphia, University of Pennsylvania School of Medicine, Philadelphia, Pennsylvania 19104-4318

Received November 26, 2007; Revised Manuscript Received December 13, 2007

ABSTRACT: The tertiary structure of apolipoprotein (apo) A-I and the contributions of structural domains to the properties of the protein molecule are not well defined. We used a series of engineered human and mouse apoA-I molecules in a range of physical−biochemical measurements to address this issue. Circular dichroism measurements of α-helix thermal unfolding and fluorescence spectroscopy measurements of 8-anilino-1-napthalenesulfonic acid binding indicate that removal of the C-terminal 54 amino acid residues from human and mouse apoA-I has similar effects; the molecules are only slightly destabilized, and there is a decrease in hydrophobic surface exposure. These results are consistent with both human and mouse apoA-I adopting a two-domain tertiary structure, comprising an N-terminal antiparallel helix bundle domain and a separate less ordered C-terminal domain. Mouse apoA-I is significantly less resistant than human apoA-I to thermal and chemical denaturation; the midpoint of thermal unfolding of mouse apoA-I at 45 °C is 15 °C lower and the midpoint of guanidine hydrochloride denaturation ($D_{1/2}$) occurs at 0.5 M as compared to 1.0 M for human apoA-I. These differences reflect the overall greater stability of the helix bundle formed by residues 1−189 in human apoA-I. Measurements of the heats of binding to egg phosphatidylcholine (PC) small unilamellar vesicles and the kinetics of solubilization of dimyristoyl PC multilamellar vesicles indicate that the more stable human helix bundle interacts poorly with lipids as compared to the equivalent mouse N-terminal domain. The C-terminal domain of human apoA-I is much more hydrophobic than that of mouse apoA-I; in the lipid-free state the human C-terminal domain (residues 190−243) is partially α-helical and undergoes cooperative unfolding ($D_{1/2} = 0.3$ M) whereas the isolated mouse C-terminal domain (residues 187−240) is disordered in dilute solution. The human C-terminal domain binds to lipid surfaces much more avidly than the equivalent mouse domain. Human and mouse apoA-I have very different tertiary structure domain contributions for achieving functionality. It is clear that the stability of the N-terminal helix bundle, and the hydrophobicity and α-helix content of the C-terminal domain, are critical factors in determining the overall properties of the apoA-I molecule.

There is considerable interest in understanding the structure−function relationships of human apolipoprotein (apo) A-I because of the important anti-atherogenic properties that the molecule displays. The latter properties are reflected in the fact that apoA-I is the principal protein of high-density lipoprotein (HDL[1]) and elevated levels of plasma HDL are associated with a reduced incidence of coronary artery disease (*1*). The protective functions of HDL and apoA-I arise, at least in part, because of their participation in the reverse transport of cholesterol from peripheral cells to the liver for excretion from the body (*2*). The ability of the apoA-I molecule to bind to lipids and cell surface receptors (*3*, *4*) is central to its role in mediating this cholesterol transport, and it is important to understand the structural basis for these effects.

The mature human apoA-I molecule in plasma contains 243 residues in a single polypeptide chain that contains 11- and 22-residue repeat amphipathic α-helices frequently separated by proline-containing segments (*5*, *6*). While the functional consequences of the secondary structure of the apoA-I molecule have been investigated in detail, the tertiary structure is less well understood because of the conformational plasticity and molten globule characteristics of the molecule in the lipid-free state (*7*). However, recently it has been demonstrated that the human apoA-I molecule folds into two tertiary structure domains (*8*−*10*). These domains comprise an N-terminal antiparallel α-helix bundle (cf. (*11*, *12*)) spanning residues 1−187 and a separate less organized

[†] This research was supported by NIH grant HL22633, the Takeda Science Foundation, and a grant-in-aid (No. 18790034) from the Japanese Ministry of Education, Culture, Sports, Science and Technology.

* To whom correspondence should be addressed: The Children's Hospital of Philadelphia, Abramson Research Center, Suite 1102, 3615 Civic Center Blvd., Philadelphia, PA 19104-4318. Telephone (215) 590-0587. Fax: (215) 590-0583. E-mail: phillipsmi@email.chop.edu.

[‡] Kobe Pharmaceutical University.

[§] University of Pennsylvania School of Medicine.

[1] Abbreviations: ANS, 8-anilino-1-napthalenesulfonic acid; apo, apolipoprotein; CD, circular dichroism; DMPC, dimyristoylphosphatidylcholine; GdnHCl, guanidine hydrochloride; HDL, high density lipoprotein; ITC, isothermal titration calorimetry; MLV, multilamellar vesicles; PC, phosphatidylcholine; SUV, small unilamellar vesicles; WT, wild type; Trp, tryptophan.

10.1021/bi702332b CCC: $40.75
Published on Web 01/19/2008

C-terminal region spanning the remainder of the molecule. The links between the structural properties of these domains and the function of the apoA-I molecule remain to be elucidated. Indeed, it is not known if the two-domain tertiary structure is a general characteristic of apoA-I or is peculiar to the human apoA-I molecule. Alignment of the amino acid sequences of different species of apoA-I indicates that there is a great deal of similarity with stretches of 22 residues separated by proline residues being a highly conserved feature (*6*). Thus, the repeating amphipathic α-helix secondary structure motif is a feature of many species of apoA-I (*6*), but it is not known if they form a N-terminal helix bundle and separate C-terminal domain. For example, the mouse apoA-I is known to exhibit different properties to human apoA-I; despite 65% amino acid identity (*6*), mouse apoA-I is less resistant to guanidine hydrochloride (GdnHCl) denaturation (*13*, *14*) and self-associates less (*13*, *15*) than human apoA-I. It is not known if these variations are a consequence of different tertiary structures in human and mouse apoA-I. Furthermore, the lipid binding properties of human and mouse apoA-I are different in that they form HDL particles of different sizes; the mouse protein forms a single population of larger HDL particles whereas human apoA-I forms two subpopulations, HDL_2 and HDL_3 (*15*, *16*). Thus, understanding the differences in the structure−function relationships of human and mouse apoA-I will provide significant insights into how this protein mediates cholesterol transport and exerts antiatherogenic effects.

Here, we use physical−biochemical measurements on human and mouse apoA-I variants to establish that, like the human protein, mouse apoA-I adopts a two-domain tertiary structure in the lipid-free state. Examination of the separate N- and C-terminal domains in human and mouse apoA-I indicates that the characteristics of these domains are different in the two proteins, and that the properties of apoA-I are critically affected by the stability of the N-terminal helix bundle and the hydrophobicity of the C-terminal domain.

EXPERIMENTAL PROCEDURES

ApoA-I Variants. Murine apoA-I cDNA (kindly provided by Dr. Anantharamaiah) was modified (by introducing the mutations Q225K/V226A) to the sequence presented in the GenBank accession number NCBI NM_009692 that encodes mouse apoA-I protein as defined in Swiss-Prot entry Q00623. This cDNA was cloned into the pET32a(+) vector from Novagen to express the wild-type (WT) mouse apoA-I protein as a His-tagged thioredoxin fusion protein (*8*, *17*). ApoA-I cDNA encoding mouse apoA-I amino acids 1−186 was generated by PCR from intact murine apoA-I cDNA and cloned into the pET32a(+) vector with primers 5′-cgggatccgatgaaccgcagtcccaatg-3′ and 5′-ggaattctcacaaggtagggttgctcttg-3′. A cDNA insert encoding mouse apoA-I amino acids 187−240 was engineered from the cloned murine apoA-I cDNA pET32a(+) plasmid using the QuickChange site-directed mutagenesis kit (Stratagene, CA) and the following primers: 5′- ggtaccacgcggatccaacgagtaccacacc -3′ and 5′-ggtgtggtactcgttggatccgcgtggtacc -3′. Similarly human apoA-I cDNA encoding amino acids 190−243 was cloned from a pET32a(+) expression vector containing human apoA-I cDNA (*8*) using the following primers: 5′-ggtaccacgcggatccgccgagtaccacgccaagg -3′ and 5′- ccttgcgtggtactcggcggatccgcgtggtacc -3′. Human/mouse and mouse/human apoA-I hybrid molecules were engineered using the Stratagene "domain-swap" protocol where the domain to be swapped was first PCR-amplified, gel purified and then used as the megaprimer in the subsequent QuickChange site-directed mutagenesis.

The human and mouse apoA-I variants encoded by these cDNA inserts were expressed and purified according to previously published procedures (*8*, *17*). Cleavage of the thioredoxin fusion protein with thrombin leaves the target apoA-I with two extra amino acids, Gly-Ser, at the amino terminus. The apoA-I preparations were at least 95% pure as assessed by SDS-PAGE and protein concentrations were determined by a Lowry procedure or absorbance at 280 nm.

Spectroscopy. Far-UV CD spectra were obtained as described before (*8*, *18*) to determine the α-helix contents of the apoA-I variants. Near-UV CD spectra were obtained by scanning over the wavelength range 270−320 nm using a 1 cm cuvette. The parameters describing the reversible thermal denaturation were obtained by monitoring the molar ellipticity at 222 nm over the temperature range 20−90 °C (*8*). Similarly, the parameters describing the reversible chemical denaturation (*19*) were determined by monitoring the molar ellipticity at 222 nm after samples were incubated with given concentrations of GdnHCl overnight at 4 °C (*18*). To determine the influence of lipid binding on the α-helix content of apoA-I, the protein was incubated for 1 h with excess egg phosphatidylcholine (PC) small unilamellar vesicles (SUV) before the CD spectrum was recorded (*20*).

The fluorescence emission spectra from 300 to 400 nm of the tryptophan (Trp) residues in apoA-I samples treated with increasing concentrations of GdnHCl were used to calculate the free energy and midpoint of denaturation, as described before (*8*). To monitor the exposure of Trp residues, the quenching of the fluorescence emission spectra by increasing concentrations of KI was determined. To monitor the exposure of hydrophobic surface, 8-anilino-1-napthalenesulfonic acid (ANS) fluorescence spectra were collected from 400 to 600 nm at an excitation wavelength of 395 nm in the absence and presence of the apoA-I variants and analyzed as described previously (*8*).

Lipid Interactions. Heats of binding of apoA-I to egg PC SUV were measured by isothermal titration calorimetry (*20*). The abilities of the apoA-I variants to solubilize dimyristoyl PC (DMPC) multilamellar vesicles (MLV) were compared by monitoring the decrease in absorbance at 325 nm (*21*). The 10 min timecourses were fitted to a monoexponential decay equation. The 10 min decrease in absorbance was measured as a function of apoA-I concentration to obtain K_m and V_{max} values.

RESULTS

Two-Domain Tertiary Structure in Human and Mouse apoA-I. In agreement with previous results (*8*), the data in Table 1 indicate that the recombinant WT human apoA-I is about 44% α-helical in dilute solution. While the α-helical segments in the region spanning residues 1−98 (*22*), and in the C-terminal domain have been defined (*23*), the identities of all 108 α-helical residues are not known precisely. However, it is established that there are two tertiary structure domains in the human apoA-I molecule; residues 1−189 form an N-terminal antiparallel helix bundle while residues

Table 1: α-Helix Content and Thermal Denaturation Parameters of Human and Mouse ApoA-I Variants

	α-helix[a] (%)	number of residues		T_m[c] (°C)	ΔH_v[d] (kcal/ mol)
		in protein[b]	in helix		
human WT	44 ± 4	245	108	60	33
human (1−189)	51 ± 2	191	97	56	49
human (190−243)	33 ± 3	56	18	51	33
mouse WT	36 ± 5	242	87	45	52
mouse (1−186)	37 ± 3	188	70	41	39
mouse (187−240)	14 ± 1	56	8	-	-

[a] Mean ± SD from at least three independent experiments. [b] The numbers of amino acids include the Gly-Ser present at the amino terminus in the engineered apoA-I molecules. [c] The reproducibility in midpoint temperature T_m is ±1.5 °C. [d] Van't Hoff enthalpy: estimated error is ±0.5 kcal/mol.

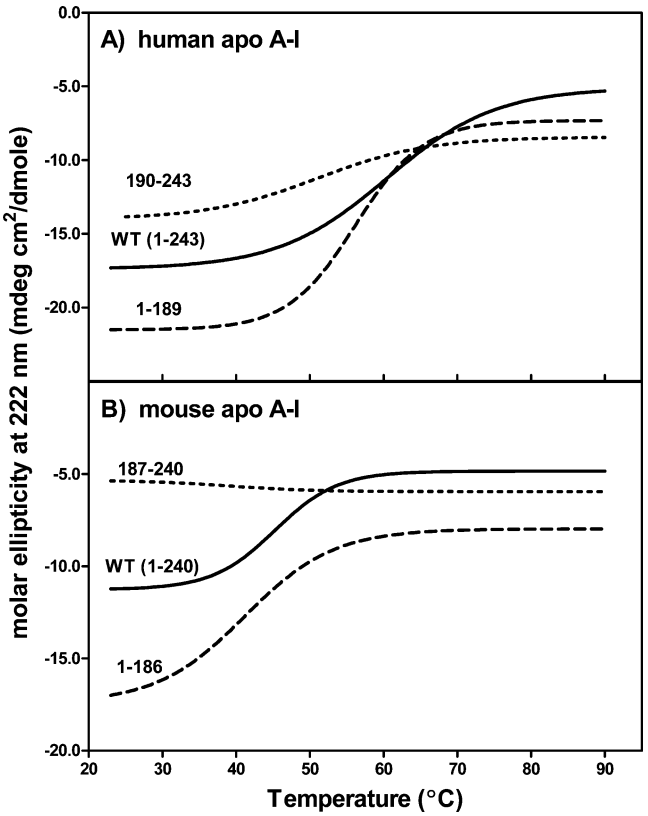

FIGURE 1: Thermal unfolding of wild-type (WT) human and mouse apoA-I and their N-terminal and C-terminal domains monitored by the ellipticity at 222 nm. A. Human apoA-I. The N-terminal domain encompasses residues 1−189 and the C-terminal domain spans the remaining residues 190−243. B. Mouse apoA-I. The N-terminal domain encompasses residues 1−186 and the C-terminal domain spans the remaining residues 187−240.

190−243 form a separate, less ordered domain (*8*). A high-resolution crystal structure has defined this two domain structure for the ∼ 80% α-helical apoA-I molecule in a highly concentrated state (*10*). The effects of removing the C-terminal domain on the properties of the human apoA-I molecule provide evidence for the two-domain structure in dilute solution. Thus, removal of 54 amino acids (residues 190−243) would be expected to cause a major disruption of the apoA-I molecule if it were folded into a single domain. However, the facts that the thermal denaturation is not affected much (compare the results for human WT apoA-I and apoA-I (1−189) in Figure 1A and Table 1), and that the degree of hydrophobic surface exposure (as reflected by ANS binding, Table 2) is decreased rather than increased by elimination of the C-terminal domain, are consistent with the existence of a two-domain tertiary structure. This conformation is similar to that adopted by apoE and is also indicated by cross-linking and mass spectrometry studies of human apoA-I in dilute solution (*9*).

Does mouse apoA-I (which is three amino acids shorter than human apoA-I) also adopt a 2-domain tertiary structure similar to that of human apoA-I? Under the same experimental conditions, the α-helix content of mouse apoA-I is 36% as compared to 44% for human apoA-I (Table 1). Furthermore, from the thermal denaturation curves in Figure 1 it is apparent that mouse apoA-I is less stable; the midpoint of 45 °C is 15° lower than that of human apoA-I (Table 1). However, inspection of the thermal denaturation results (Figure 1) and ANS fluorescence data (Table 2) reveals that removal of the C-terminal region (residues 187−240) from WT mouse apoA-I has qualitatively similar consequences to those described above for removing residues 190−243 from human apoA-I. Thus, it can be inferred that residues 1−186 in mouse apoA-I are involved in formation of a helix bundle while residues 187−240 are organized into a separate domain.

The C-terminal domains in WT human and mouse apoA-I exhibit strikingly different properties. The isolated human apoA-I (190−243) molecule is one-third α-helical and undergoes cooperative thermal denaturation with a T_m of 51 °C (cf. (*24*)) (Figure 1A and Table 1). In contrast, mouse apoA-I (187−240) does not exhibit any cooperative unfolding upon heating (Figure 1B), consistent with the molecule being essentially in a random coil conformation in solution (Table 1). Consistent with the mouse C-terminal domain being much more disordered than the human counterpart, human apoA-I (190−243) induces a relative ANS fluorescence intensity of 1.1 as compared to a value of 0.3 for mouse apoA-I (187−240) (Table 2). This factor presumably underlies the elevated ANS fluorescence intensity observed with WT human apoA-I relative to WT mouse apoA-I (Table 2).

N-Terminal Domain Organization. The fact that removal of the C-terminal domain has opposite effects on the cooperativity of thermal denaturation in human and mouse apoA-I (see the Van't Hoff enthalpies in Table 1) suggests that the cooperativity of helix packing in the human N-terminal domain is decreased by interaction with the C-terminal domain whereas the opposite effect occurs in mouse apoA-I. We took advantage of the fact that all the Trp residues are located in the N-terminal helix bundle domain (positions 8, 50, 72, and 108 in human apoA-I and positions 7, 49, 71, 80, and 107 in mouse apoA-I) by using Trp fluorescence to compare the packing in this region of the two proteins. The wavelengths of maximum fluorescence are about 336 and 339 nm for WT human and mouse apoA-I, respectively, indicative of a more polar environment for the Trp residues in mouse apoA-I. KI fluorescence quenching experiments (data not shown) indicate that the Trp residues are relatively more exposed to the aqueous phase in mouse apoA-I than in human apoA-I. This result is consistent with the observation that the amount of hydrophobic surface exposure (as monitored by ANS binding, Table 2) is greater in mouse apoA-I (1−186) than in human apoA-I (1−189).

The orientational ordering of the Trp residues was also examined by obtaining the near-UV CD spectra shown in

Table 2: Parameters of GdnHCl-Induced Denaturation and ANS Binding of ApoA-I Variants

	molar ellipticity			fluorescence intensity			
	$\Delta G°_D$ (kcal/mol)	m	$D_{1/2}$ (M)	$\Delta G°_D$ (kcal/mol)	m	$D_{1/2}$ (M)	ANS fluorescence[a]
human WT	3.5 ± 0.2	3.5 ± 0.2	1.0 ± 0.1	3.1 ± 0.3	2.9 ± 0.2	1.06 ± 0.04	1.0
human 1−189	4.5 ± 0.2	4.5 ± 0.2	1.0 ± 0.1	3.4 ± 0.1	3.2 ± 0.1	1.05 ± 0.05	0.6
human 190−243	1.0 ± 0.1	3.7 ± 0.2	0.3 ± 0.04	-	-	-	1.1
mouse WT	2.4 ± 0.2	4.3 ± 0.4	0.55 ± 0.1	2.0 ± 0.1	3.2 ± 0.1	0.62 ± 0.04	0.85
mouse 1−186	1.7 ± 0.2	3.4 ± 0.3	0.5 ± 0.1	1.9 ± 0.1	3.3 ± 0.1	0.58 ± 0.04	0.7
mouse 187−240	-	-	-	-	-	-	0.3

[a] Values are relative to WT. Estimated error is within ±0.1.

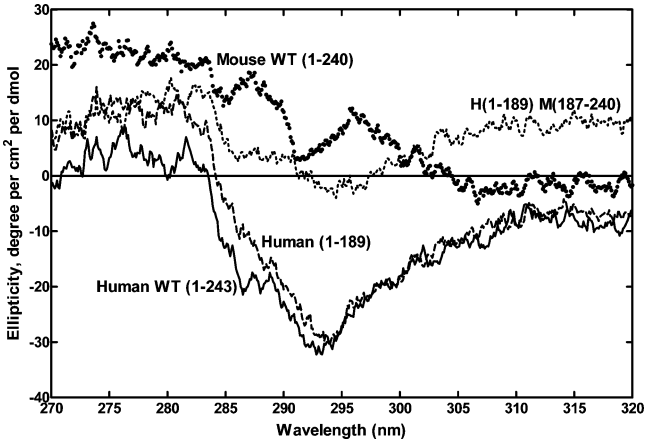

FIGURE 2: Near-UV CD spectra of human and mouse apoA-I variants. The spectra (averaged over 16 accumulations) were obtained at room temperature at a protein concentration of 0.3 mg/mL: the spectrum for the buffer alone (10 mM sodium phosphate, pH 7.4) was subtracted.

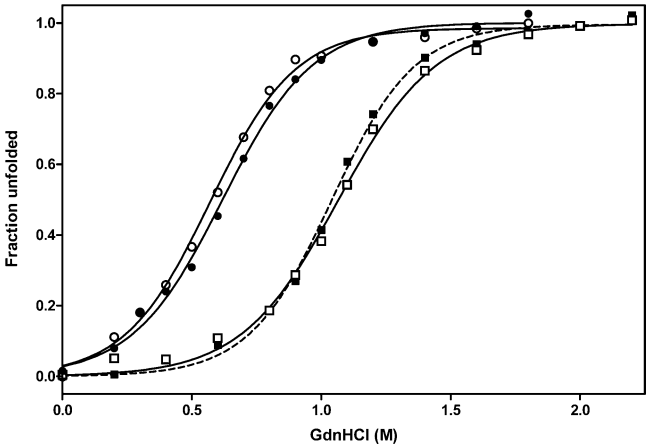

FIGURE 3: GdnHCl-induced denaturation of human and mouse apoA-I monitored by Trp fluorescence. Human WT (□), human (1−189) (■), mouse WT (○), mouse (1−186) (●).

Figure 2. Consistent with a prior report (*7*), the spectrum of WT human apoA-I at room-temperature exhibits a pronounced negative trough with a minimum at 292 nm, indicating some orientational ordering of the Trp residues. The trough is similar in the spectrum of human apoA-I (1−189), indicating that this ordering is maintained in the isolated human N-terminal domain. In striking contrast, there is no negative trough in the spectrum of WT mouse apoA-I, indicating that the Trp residues are disordered in this case. The spectra for mouse apoA-I (1−186) and the hybrid apoA-I molecule, mouse (1−186) human (190−243), are similar (data not shown), indicating that, in all cases, the N-terminal domain of mouse apoA-I is relatively disordered. This conclusion is consistent with the increased hydrophobic surface exposure observed with this domain (see above). Interestingly, the negative trough at 292 nm is also missing in the spectrum of the hybrid apoA-I human (1−189) mouse (187−240) (Figure 2); this result shows that the Trp residues are disordered in the human N-terminal domain in this situation. It follows that while removal of the C-terminal domain from WT human apoA-I does not alter the Trp packing, substitution of the mouse C-terminal domain disorders the human N-terminal helix bundle to some extent.

Stabilities of N-Terminal Helix Bundle Domains in Human and Mouse ApoA-I. As mentioned above, changes in Trp fluorescence monitor alterations in packing in the N-terminal helix bundle domain of apoA-I. Thus, the effects of increasing GdnHCl concentrations on Trp fluorescence (Figure 3) indicate that the helix bundle domain in both human and mouse apoA-I unfolds cooperatively. Mouse apoA-I is less stable than the human protein with the midpoints of denaturation occurring at 0.6 and 1.0 M GdnHCl, respectively (Table 2) (cf. refs *13*, *14*). Removal of the C-terminal domain from either human or mouse apoA-I does not significantly alter the stability of the N-terminal helix bundle domain (Figure 3 and Table 2). This lack of an effect on stability by removal of the C-terminal domain suggests that the induced alterations in helix packing and hydrophobic residue exposure in the helix bundle domain discussed above are less important for helix bundle stability than other interactions such as interhelical salt-bridges.

The CD results in Figure 4 for WT human apoA-I show that the α-helix unfolding induced by GdnHCl occurs with a midpoint of 1.0 M, consistent with the results of the equivalent Trp fluorescence experiments (Table 2). The α-helices in the isolated human C-terminal domain are relatively unstable and unfold with a midpoint of 0.3 M GdnHCl (Figure 4 and Table 2). Removal of the α-helices in this domain from WT human apoA-I does not affect the stability of the helices in the N-terminal domain (Figure 4); this is consistent with the near-UV CD data in Figure 2 showing that this deletion does not affect the packing of the Trp residues in the N-terminal domain. The α-helices in WT mouse apoA-I unfold at a lower GdnHCl concentration ($D_{1/2}$ = 0.55 M) but in a similarly cooperative fashion (similar m value) as compared to human apoA-I (Table 2). This destabilization is not a consequence of the presence of the disordered and polar C-terminal domain in mouse apoA-I because the isolated mouse apoA-I (1−186) domain unfolds similarly to WT mouse apoA-I when exposed to GdnHCl (Figure 4 and Table 2).

ApoA-I Binding to Stable Egg PC SUV. Both WT human and mouse apoA-I bind to egg PC SUV with large exother-

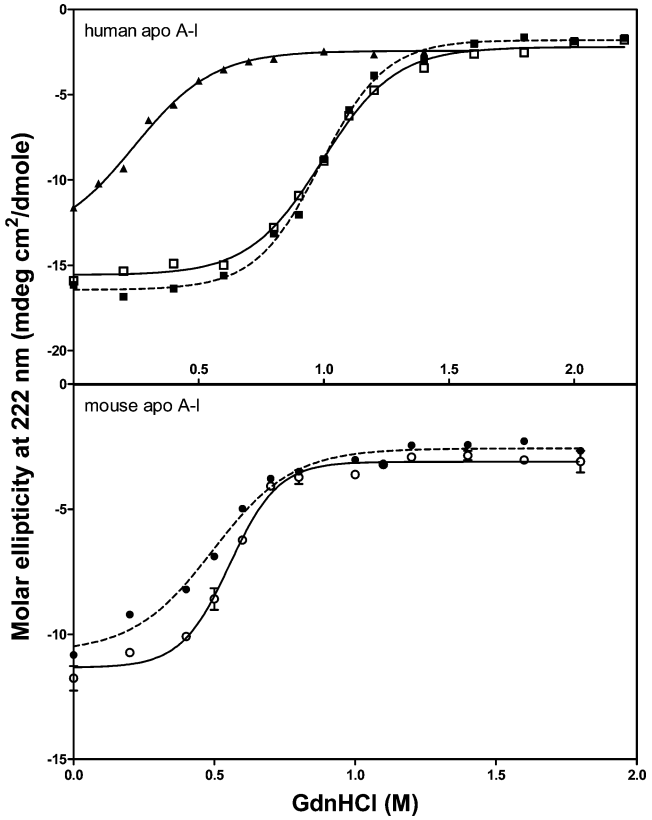

FIGURE 4: GdnHCl-induced denaturation of human and mouse apoA-I monitored by molar ellipticity. (A) Human apoA-I: WT (□), (1−189) (■), (190−243) (▲). (B) Mouse apoA-I: WT (○), (1−186) (●).

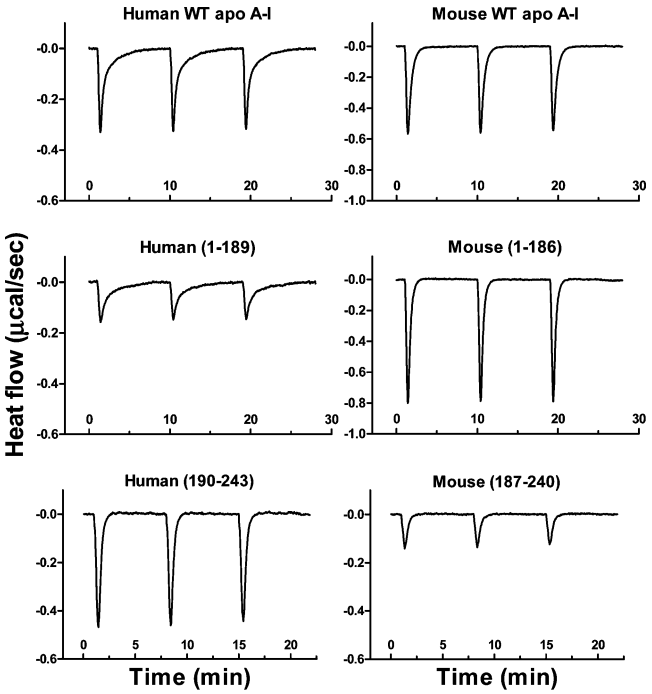

FIGURE 5: Isothermal titration calorimetry traces for binding of human and mouse apoA-I to egg PC SUV. An 8 μL amount of protein solution (0.8 mg/mL) was injected into SUV (PC concentration 15 mM) at 25 °C.

mic heats of about −100 kcal/mol (Figure 5 and Table 3). As reported before, when human apoA-I binds to SUV, there is an increase in α-helix content (Figure 6), and this conformational change gives rise to a large part of the exothermic enthalpy change (*20*, *25*). The CD spectra in Figure 6 indicate that there is a similar increase in α-helix content (∼60 residues, Table 3) when WT mouse apoA-I binds to the SUV. Strikingly, despite the overall similarity in the energetics of binding of WT human and mouse apoA-I, the energetics of binding of the separate human and mouse N- and C-terminal domains are very different. Thus, the human N-terminal domain exhibits an enthalpy of −39 kcal/mol (a reduction of 53 kcal/mol relative to WT apoA-I) whereas the mouse N-terminal domain gives an enthalpy of −88 kcal/ mol (a reduction of only 19 kcal/mol relative to WT mouse apoA-I) (Table 3). As expected, the larger heat for the mouse N-terminal domain is associated with a larger increase in the number of helical residues upon lipid binding (47 as compared to 23 residues for the human N-terminal domain, Table 3). The situation is reversed for the C-terminal domains with the heat being larger for the human protein; the changes in α-helix content upon lipid binding (Table 3) are consistent with these observations.

The kinetics of interaction of human and mouse apoA-I, and their domains are also different. Inspection of the isothermal titration calorimetry curves (Figure 5) indicates that for the mouse proteins containing the N-terminal helix bundle domain, the heat decay is more rapid than for the human counterparts. This conclusion is confirmed by the halftime ($t_{1/2}$) values obtained by fitting to a monoexponential

Table 3: Parameters of Binding of ApoA-I Variants to Egg PC SUV

	ITC parameters		increase in α-helical residues[c] (amino acids)
	ΔH[a] (−kcal/mol)	half-time of decay[b] (min)	
human WT	92.6 ± 5.3	0.55	61
human 1−189	39.2 ± 2.8	0.81	23
human 190−243	18.1 ± 1.6	0.18	11
mouse WT	107.4 ± 4.3	0.31	68
mouse 1−186	88.5 ± 3.0	0.22	47
mouse 187−240	1.5 ± 0.8	0.22	3

[a] Mean ± SD from at least four measurements. [b] The halftimes of heat decay were obtained by fitting the titration curves (Figure 5) to a one-phase exponential decay model. [c] Determined from increase in apoA-I α-helix content on binding to SUV (cf. Figure 6).

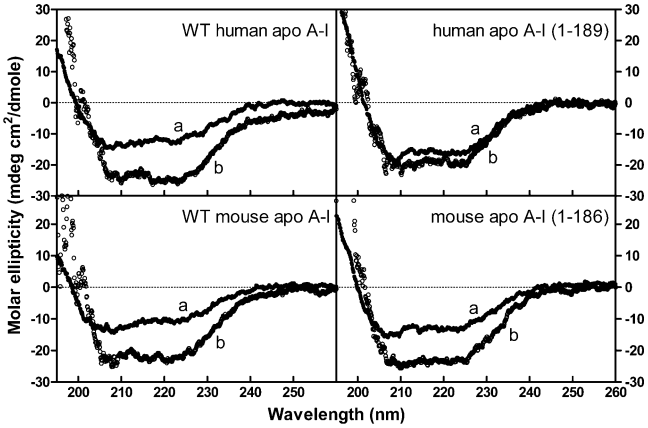

FIGURE 6: Far-UV CD spectra of human and mouse apoA-I in the absence and presence of egg PC SUV. The protein concentration was 25 or 50 μg/mL. SUV were added at a PC/protein weight ratio of 40−60/1, and the mixture was incubated for 1 h. Top: Human apoA-I (WT) and (1−189) in the absence (a) or presence (b) of SUV. Bottom: Mouse apoA-I (WT) and (1−186) in the absence (a) or presence (b) of SUV.

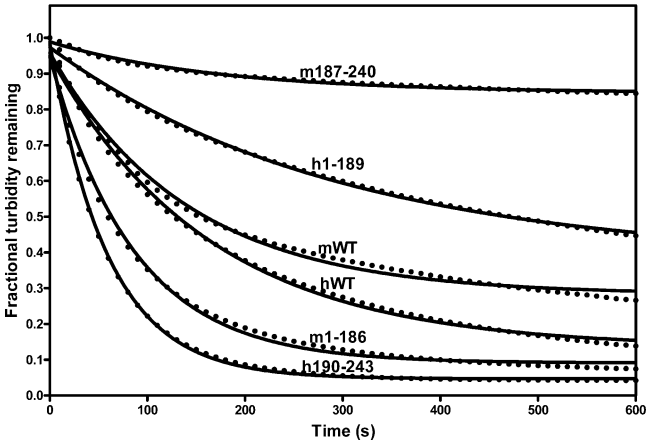

FIGURE 7: Solubilization of DMPC MLV by human and mouse apoA-I and their N- and C-terminal domains. Representative timecourses of the decrease in absorbance at 325 nm (recorded every 2s) when DMPC MLV (0.25 mg/mL) were incubated with 0.3 mg/mL protein for 10 min at 24.0 ± 0.1 °C. The measured absorbance values (solid circles) were fitted to a monoexponential decay equation (continuous lines).

Table 4: Kinetic Parameters for Solubilization of DMPC MLV by Human and Mouse ApoA-I Domains[a]

apoA-I	K_m[b] (μM)	V_{max}[b] (10 min decrease in A_{325})
human WT	1.9 ± 0.1	0.60 ± 0.01
human (1−189)	6.0 ± 0.6	0.47 ± 0.02
human (190−243)	2.6 ± 0.3	0.54 ± 0.02
mouse WT	2.8 ± 0.4	0.45 ± 0.02
mouse (1−186)	2.3 ± 0.1	0.68 ± 0.01
mouse (187−240)[c]	-	-

[a] Parameters obtained by fitting the clearance rates (Figure 7) measured as a function of protein concentration to the Michaelis−Menten equation. [b] Mean ± SE from two to four independent experiments each performed in triplicate. [c] Results did not fit Michaelis−Menten equation.

decay equation. The $t_{1/2}$ is ∼2 times shorter for WT mouse apoA-I than for WT human apoA-I, and 4 times shorter for the isolated N-terminal domains (Table 3). These results indicate that the rate of lipid binding is affected by the stability of the helix bundle domain with the less stable mouse domain binding more rapidly. The isolated human and mouse C-terminal domains both bind rapidly and with similar short $t_{1/2}$ values (Table 3).

Solubilization of DMPC MLV by ApoA-I. As is well-known, besides binding to the stable phospholipid bilayers in egg PC SUV, human apoA-I can bind to unstable DMPC bilayers in MLV and at 24° rapidly solubilize them to form discoidal HDL particles (*21*, *26*, *27*). The clearance curves in Figure 7 indicate that mouse apoA-I can solubilize DMPC MLV similarly to human apoA-I. Measurements of the clearance kinetics at different concentrations of WT human and mouse apoA-I show that both proteins exhibit similar K_m values, but the V_{max} for WT human apoA-I is about one-third higher (Table 4). As was observed with the interactions of the human and mouse proteins with egg PC SUV, the human and mouse N- and C-terminal domains exhibit quite different lipid-binding characteristics, as reflected in their abilities to solubilize DMPC MLV. Thus, the isolated human N-terminal domain is much less effective than WT human apoA-I in solubilizing DMPC MLV whereas the isolated mouse N-terminal domain is much more efficient than WT mouse apoA-I (Figure 7). This difference is reflected in both the K_m and V_{max} values listed in Table 4. These parameters also indicate that the isolated mouse N-terminal domain solubilizes DMPC MLV with higher affinity (lower K_m), and at a higher rate (higher V_{max}), than the isolated human N-terminal domain. The isolated human and mouse apoA-I C-terminal domains also exhibit strikingly different capabilities of solubilizing DMPC MLV. The mouse C-terminal domain is practically inactive whereas the human C-terminal domain is extremely effective (Figure 7). Indeed, the closeness of the concentration-dependence curves for human WT apoA-I and its C-terminal domain (Table 4) indicates that essentially all the lipid-solubilizing capability of WT human apoA-I resides in the C-terminal domain.

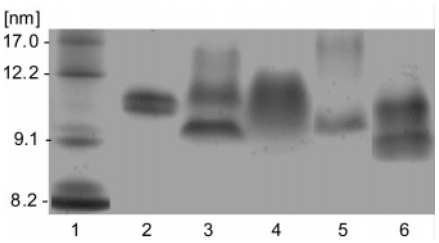

FIGURE 8: Native polyacrylamide gradient (2−36%) gel stained with Coomassie Brilliant Blue comparing the sizes of discoidal complexes with DMPC formed by human and mouse apoA-I tertiary structure domains. The proteins at a ratio of 2.5/1 w/w DMPC/apoA-I were incubated with DMPC SUV under temperature conditions (cycled three times between 10 and 37 °C) where WT human apoA-I forms a homogeneous discoidal complex (hydrodynamic diameter = 11.0 ± 0.5 nm). Lane 1, standard proteins of known hydrodynamic diameter. Lane 2, WT human apoA-I. Lane 3, human N-terminal domain, residues 1−189. Lane 4, human C-terminal domain, residues 190−243. Lane 5, WT mouse apoA-I. Lane 6, mouse N-terminal domain, residues 1−186.

Besides the variations in the rates at which human and mouse apoA-I and their isolated tertiary structure domains can solubilize DMPC MLV, these proteins also create different sizes of discoidal complexes with DMPC. Thus, under conditions where WT human apoA-I forms homogeneous discoidal particles (hydrodynamic diameter = 11 ± 0.5 nm), WT mouse apoA-I forms two sizes of particles (diameters = 10 and 17 nm) (Figure 8). The gel depicted in Figure 8 also demonstrates that the isolated N-terminal domains of both human and mouse apoA-I form two sizes of discoidal particles; the particles containing the mouse protein are consistently smaller (by about 1 nm). The discoidal particles formed by the isolated human C-terminal domain migrate in the gel as a diffuse broad band (Figure 8); the diameter of these particles is 11 ± 1 nm, which is similar to that of WT apoA-I/DMPC complexes (cf. (*24*)). In contrast, the isolated mouse apoA-I C-terminal domain cannot solubilize the DMPC MLV to create discoidal particles (Figure 7).

Effects of Exchanging the N- and C-Terminal Domains between Human and Mouse ApoA-I. To confirm the influence of domain properties on apoA-I structure and function, we extended the studies of the N- and C-terminal domains of the human and mouse proteins by preparing some domain-swap, hybrid molecules. As shown in Table 5, replacement of the C-terminal domain of human apoA-I with the equivalent mouse domain to create the hybrid apoA-I H(1−189)M(187−240) leads to no change in α-helix content. The ANS fluorescence results indicate that there is decreased

Table 5: Stabilities and Lipid-Binding Properties of N- and C-Terminal Domain-Swap Human (H) and Mouse (M) Hybrid ApoA-I Molecules

	structure		stability		lipid interaction: DMPC clearance[e]	
apoA-I	α-helix[a] (%)	ANS fluorescence intensity[b]	T_m (°C)[c]	$\Delta G°$ (kcal/ mol)[d]	K_m (μM)	V_{max} (10 min decrease in A_{325})
human WT	44 ± 4	1.0	60	3.1 ± 0.3	1.9 ± 0.1	0.60 ± 0.01
H (1−189) M (187−240)	45 ± 2	0.8	54	2.3 ± 0.1	5.3 ± 0.5	0.70 ± 0.04
mouse WT	36 ± 5	0.85	45	2.0 ± 0.1	2.8 ± 0.4	0.45 ± 0.02
M (1−186) H (190−243)	39 ± 2	1.6	50	2.4 ± 0.1	1.7 ± 0.3	0.62 ± 0.04

[a] Mean ± SD measured by CD at 50 μg/mL. [b] Values are measured at 50 μg protein/mL and are ratios to WT apoA-I. Error is within 0.1. [c] Midpoint of thermal denaturation measured by CD (±1.5 °C). [d] Free energy of denaturation by guanidine HCl as measured by Trp fluorescence. [e] Kinetic parameters for solubilization of DMPC MLV (cf. Table 4). Mean ± SE.

hydrophobic surface exposure due to replacement of the hydrophobic human C-terminal domain with the more polar and disordered mouse C-terminal domain (Table 5). The overall stability of this hybrid molecule is decreased relative to WT human apoA-I, as reflected by the 6 °C decrease in the T_m (from 60° to 54 °C) of thermal unfolding of the α-helices. In agreement with this, GdnHCl denaturation as monitored by Trp fluorescence indicates that the presence of the mouse C-terminal domain in the hybrid molecule destabilizes the human helix-bundle domain (Table 5). This result is consistent with the near-UV CD results of Figure 2 where the same substitution is shown to induce a loss of Trp orientational ordering. Comparison of the properties of apoA-I H (1−189) M (187−240) with WT mouse apoA-I provides insight into the effects of N-terminal domain exchange. The structural and stability properties of this hybrid generally reflect the greater stability of the human apoA-I helix bundle. The DMPC solubilization results indicate that introduction of the human helix bundle domain reduces the affinity of the lipid interaction. Notably, substitution of the mouse C-terminal domain causes a similar increase in the K_m for DMPC MLV solubilization to that caused by deletion of the C-terminal domain from WT human apoA-I (Table 4). This decrease in the affinity of the interaction with lipid is consistent with the model in which the C-terminal domain is important in the initial step of lipid binding (*8*, *23*), with the hydrophobicity of this domain being critical.

There are also striking alterations in properties of the reverse hybrid, apoA-I M (1−186) H (190−243), created by replacing the C-terminal domain of mouse apoA-I with the human counterpart. This hybrid molecule is more stable than WT mouse apoA-I (Table 5), consistent with interaction between the more hydrophobic human C-terminal domain and the mouse N-terminal helix bundle stabilizing the latter more than the equivalent domain−domain interaction in WT mouse apoA-I. The relative ANS fluorescence of 1.6 for this hybrid molecule is high relative to WT human apoA-I (Table 5). This result suggests that the human C-terminal domain interacts differently (compared to the equivalent mouse domain) with the mouse N-terminal helix bundle domain, leading to greater hydrophobic surface exposure. As expected, addition of the hydrophobic human C-terminal domain to the mouse N-terminal helix bundle domain gives a hybrid apoA-I that exhibits a higher affinity solubilization of DMPC MLV.

DISCUSSION

The similar effects of deletion of the C-terminal domain on the properties of human and mouse apoA-I are consistent with the latter protein adopting a two-domain tertiary structure, analogous to that adopted by human apoA-I and apoE (*8*). In this model of WT mouse apoA-I tertiary structure, residues 1−186 are involved in formation of an antiparallel helix bundle while residues 187−240 are folded in a separate, disordered domain. Overall, the primary structures of human and mouse apoA-I are 65% identical, with the N- and C-terminal domains being 70% and 46% identical, respectively (*6*). Indeed, the most highly differentiated parts of the human and mouse apoA-I molecules are the C-terminal 22-residue segments that have only 30% sequence identity. The differences in amino acid sequence give rise to variations in polarity between human and mouse apoA-I. The average hydropathic index per amino acid residue (*28*) is −0.84 and −0.95 (a more negative value is more polar) for WT human and mouse apoA-I, respectively. Interestingly, the hydropathies of the human and mouse N-terminal helix bundle domains are similar but the mouse C-terminal domain has a much more negative hydropathic index (−0.72 vs −0.3 for human apoA-I (190−243)) indicating that it is much more polar. It is valuable to consider how these variations in domain characteristics influence the behavior of the apoA-I molecule.

Influence of N- and C-Terminal Domain Characteristics on ApoA-I Stability. WT human and mouse apoA-I have very different overall stabilities as reflected in their susceptibilities to thermal and GdnHCl denaturation (Figures 1, 3, and 4). The N-terminal helix bundle in human apoA-I is more stable than that in mouse apoA-I. The 15 °C higher melting temperature (Table 1) reflects the overall greater stability (under conditions where there are both electrostatic and hydrophobic contributions to the stabilization) of the helix bundle formed by residues 1−189 in human apoA-I. The fact that the free energy of unfolding measured by GdnHCl denaturation (where electrostatic interactions between amino acids are shielded by the ionic denaturant (*29*)) is also greater for the human helix bundle domain than for the equivalent mouse domain (Table 2) is consistent with there being an important hydrophobic contribution to this extra stabilization.

Besides the very different polarities of the human and mouse C-terminal domains mentioned above, results summarized in Tables 1−2 indicate that these isolated domains have different secondary structures and stabilities. Mouse apoA-I (187−240) is disordered in dilute solution whereas human apoA-I (190−243) is partially α-helical and undergoes cooperative denaturation. Comparison of the numbers of α-helical residues in the intact apoA-I molecules and their separate N- and C-terminal domains (Table 1) suggests that the difference in C-terminal domain secondary structure is

maintained in the intact apoA-I molecules. Furthermore, since the sums of the numbers of α-helical residues in the separate N- and C-terminal domains are similar, within the experimental uncertainty, to the numbers of helical residues in the intact human and mouse apoA-I molecules (Table 1), it follows that interactions between the domains cause little or no change in α-helix content. Removal of the more organized and hydrophobic C-terminal domain in human apoA-I is the reason for the bigger decrease in ANS binding compared to that seen when the equivalent deletion is made in mouse apoA-I (Table 2). However, deletion of their respective C-terminal domains induces similar changes in the overall stability of the human and mouse N-terminal helix bundle domains; both isolated N-terminal domains exhibit a T_m value that is 4 °C lower than that of the parent apoA-I molecule (Table 1). This observation is consistent with the net energetic contribution of interactions of the C-terminal with the N-terminal helix bundle domain to the stability of the latter domain being similar in the human and mouse apoA-I molecules. Interestingly, relative to the effect of the polar mouse C-terminal domain, interaction of the hydrophobic human C-terminal domain leads to greater stabilization of the WT mouse apoA-I molecule (the T_m for apoA-I M(1−186)H(190−243) is 50° compared to 45 °C for WT mouse apoA-I (Table 5)). The higher free energy of unfolding of the N-terminal domain in the hybrid molecule (as monitored by Trp fluorescence and GdnHCl denaturation) confirms that this stabilization effect includes the helix bundle domain.

Influence of N- and C-Terminal Domain Characteristics on ApoA-I Lipid Binding. Relative to the WT protein, human apoA-I (1−189) does not bind well to lipids whereas human apoA-I (190−243) binds effectively (Figures 5−7). These results indicate that the stable N-terminal helix bundle in human apoA-I interacts poorly with lipid surfaces in contrast to the hydrophobic C-terminal domain that interacts with high affinity. These results are consistent with a two-step mechanism for binding of human apoA-I to a phospholipid surface (*4*, *8*). In this model, initial binding occurs through hydrophobic amphipathic α-helices in the C-terminal domain accompanied by an increase in α-helicity probably in the region including residues 190−220 (*23*). In the second step that is slower, the N-terminal helix bundle undergoes a conformational opening thereby converting hydrophobic helix−helix interactions to helix−lipid interactions. In agreement with the idea the hydrophobic C-terminal domain controls the lipid binding of human apoA-I, the average diameters of the discoidal particles created by solubilizing DMPC are the same for the isolated C-terminal domain and WT human apoA-I, whereas the isolated N-terminal domain creates two populations of particles with different diameters (Figure 8).

While the two-step model describes the binding of human apoA-I to lipid surfaces well, it is not expected to apply to mouse apoA-I because the C-terminal domain (residues 187−240) in the latter protein is disordered and much more polar and does not bind effectively to lipids (Figures 5, 7). However, the N-terminal helix bundle (residues 1−186) that is relatively unstable in mouse apoA-I binds well to lipids (Figure 5−7). Thus, in WT mouse apoA-I the N-terminal helix bundle domain is critical for lipid binding. In this case, the unstable helix bundle can open, rapidly exposing the nonpolar faces of the amphipathic α-helices for interaction with the lipid surface. As mentioned earlier, the rate of helix bundle opening varies inversely with its stability (cf. Table 3 and discussion thereof). The open helix bundle domain of mouse apoA-I alone stabilizes two sizes of discoidal DMPC particles that are different from the two populations formed by WT mouse apoA-I (Figure 8); this indicates that, while the isolated mouse C-terminal domain cannot bind lipids, its presence in the intact apoA-I molecule modifies the lipid binding behavior of the N-terminal helix bundle domain.

SUMMARY AND CONCLUSIONS

Human and mouse apoA-I both adopt a two-domain tertiary structure that comprises an N-terminal helix bundle domain and a separate C-terminal domain. Given the phylogenetic separation between mouse and human, it is reasonable to infer that apoA-I for all higher mammals adopt a two-domain tertiary structure. Human and mouse apoA-I have very different tertiary structure domain contributions for achieving functionality. Human apoA-I functions with a relatively stable N-terminal helix bundle domain and a partially α-helical, hydrophobic C-terminal domain. Conversely, mouse apoA-I functions with an unstable N-terminal helix bundle domain and a disordered, polar C-terminal domain. Changes in both tertiary structure domains have occurred in the evolution of mouse and human apoA-I. Regarding lipid binding, the isolated mouse helix bundle domain can function effectively whereas, in the case of human apoA-I, the stability of the helix bundle precludes it from interacting well with lipid surfaces so that the presence of the hydrophobic C-terminal domain is required to initiate lipid binding. Exchanging the N- and C-terminal domains between human and mouse apoA-I gives hybrid molecules with lipid-binding properties that support this assignment of domain functions. The variations in domain contribution probably underlie the differences in HDL binding selectivity of human and mouse apoA-I. The stability of the N-terminal helix bundle as well as the hydrophobicity and α-helix content of the C-terminal domain are critical factors in determining the overall properties of apoA-I molecules, regardless of their species of origin.

REFERENCES

1. Castelli, W. P., Garrison, R. J., Wilson, P. W. F., Abbott, R. D., Kalousdian, S., and Kannel, W. B. (1986) Incidence of coronary heart disease and lipoprotein cholesterol levels, *J. Am. Med. Assoc. 256*, 2835−2838.
2. Rader, D. J. (2006) Molecular regulation of HDL metabolism and function: Implications for novel therapies, *J. Clin. Invest. 116*, 3090−3100.
3. Lund-Katz, S., Liu, L., Thuahnai, S. T., and Phillips, M. C. (2003) High density lipoprotein structure, *Front. Biosci. 8*, d1044−1054.
4. Saito, H., Lund-Katz, S., and Phillips, M. C. (2004) Contributions of domain structure and lipid interaction to the functionality of exchangeable human apolipoproteins, *Prog. Lipid Res. 43*, 350−380.
5. Segrest, J. P., Jones, M. K., De Loof, H., Brouillette, C. G., Venkatachalapathi, Y. V., and Anantharamaiah, G. M. (1992) The amphipathic helix in the exchangeable apolipoproteins: a review of secondary structure and function, *J. Lipid Res. 33*, 141−166.
6. Brouillette, C. G., Anantharamaiah, G. M., Engler, J. A., and Borhani, D. W. (2001) Structural models of human apolipoprotein A-I: a critical analysis and review, *Biochim. Biophys. Acta 1531*, 4−46.
7. Gursky, O., and Atkinson, D. (1996) Thermal unfolding of human high-density apolipoprotein A-I: implications for a lipid-free molten globular state, *Proc. Natl. Acad. Sci. U.S.A. 93*, 2991−2995.

8. Saito, H., Dhanasekaran, P., Nguyen, D., Holvoet, P., Lund-Katz, S., and Phillips, M. C. (2003) Domain structure and lipid interaction in human apolipoproteins A-I and E: A general model, *J. Biol. Chem. 278*, 23227−23232.
9. Silva, R. A. G., Hilliard, G. M., Fang, J., Macha, S., and Davidson, W. S. (2005) A three-dimensional molecular model of lipid-free apolipoprotein A-I determined by cross-linking/mass spectrometry and sequence tracking, *Biochemistry 44*, 2759−2769.
10. Ajees, A. A., Anantharamaiah, G. M., Mishra, V. K., Hussain, M. M., and Murthy, S. (2006) Crystal structure of human apolipoprotein A-I: Insights into its protective effect against cardiovascular diseases, *Proc. Natl. Acad. Sci. 103*, 2126−2131.
11. Davidson, W. S., Arnvig-McGuire, K., Kennedy, A., Kosman, J., Hazlett, T., and Jonas, A. (1999) Structural organization of the N-terminal domains of apolipoprotein A−I: Studies of tryptophan mutants, *Biochemistry 38*, 14387−14395.
12. Beckstead, J. A., Block, B. L., Bielicki, J. K., Kay, C. M., Oda, M. N., and Ryan, R. O. (2005) Combined N- and C-terminal truncation of human apolipoprotein A-I yields a folded, functional central domain, *Biochemistry 44*, 4591−4599.
13. Gong, E., Tan, C. S., Shoukry, M. I., Rubin, E. M., and Nichols, A. V. (1994) Structural and functional properties of human and mouse apolipoprotein A-I, *Biochim. Biophys. Acta 1213*, 335−342.
14. Ren, X., Zhao, L., Sivashanmugam, A., Miao, Y., Korando, L., Yang, Z., Reardon, C. A., Getz, G. S., Brouillette, C. G., Jerome, W. G., and Wang, J. (2005) Engineering mouse apolipoprotein A-I into a monomeric, active protein useful for structural determination, *Biochemistry 44*, 14907−14919.
15. Reschly, E. J., Sorci-Thomas, M., Davidson, W. S., Meredith, S. C., Reardon, C., and Getz, G. S. (2002) Apolipoprotein A-I alpha-helices 7 and 8 modulate high density lipoprotein subclass distribution, *J. Biol. Chem. 277*, 9645−9654.
16. Rubin, E. M., Ishida, B. Y., Clift, S. M., and Krauss, R. M. (1991) Expression of human apolipoprotein A-I in transgenic mice results in reduced plasma levels of murine apolipoprotein A-I and the appearance of two new high density lipoprotein size subclasses, *Proc. Natl. Acad. Sci. U.S.A. 88*, 434−438.
17. Morrow, J. A., Arnold, K. S., and Weisgraber, K. H. (1999) Functional characterization of apolipoprotein E isoforms overexpressed in escherichia coli, *Protein Expr. Purif. 16*, 224−230.
18. Tanaka, M., Dhanasekaran, P., Nguyen, D., Ohta, S., Lund-Katz, S., Phillips, M. C., and Saito, H. (2006) Contributions of the N- and C-terminal helical segments to the lipid-free structure and lipid interaction of apolipoprotein A-I, *Biochemistry 45*, 10351−10358.
19. Reijngoud, D. J., and Phillips, M. C. (1982) Mechanism of dissociation of human apolipoprotein A-I from complexes with dimyristoylphosphatidylcholine as studied by guanidine hydrochloride denaturation, *Biochemistry 21*, 2969−2976.
20. Saito, H., Dhanasekaran, P., Nguyen, D., Deridder, E., Holvoet, P., Lund-Katz, S., and Phillips, M. C. (2004) Alpha-helix formation is required for high affinity binding of human apolipoprotein A-I to lipids, *J. Biol. Chem. 279*, 20974−20981.
21. Segall, M. L., Dhanasekaran, P., Baldwin, F., Anantharamaiah, G. M., Weisgraber, K., Phillips, M. C., and Lund-Katz, S. (2002) Influence of apoE domain structure and polymorphism on the kinetics of phospholipid vesicle solubilization, *J. Lipid Res. 43*, 1688−1700.
22. Lagerstedt, J. O., Budamagunta, M. S., Oda, M. N., and Voss, J. C. (2007) EPR spectroscopy of site-directed spin labels reveals the structural heterogeneity in the N-terminal domain of apo AI in solution, *J. Biol. Chem. 282*, 9143−9149.
23. Oda, M. N., Forte, T. M., Ryan, R. O., and Voss, J. C. (2003) The C-terminal domain of apolipoprotein A-I contains a lipid-sensitive conformational trigger, *Nat. Struct. Biol. 10*, 455−460.
24. Zhu, H. L., and Atkinson, D. (2007) Conformation and lipid binding of a C-terminal (198−243) peptide of human apolipoprotein A-I, *Biochemistry 46*, 1624−1634.
25. Arnulphi, C., Jin, L., Tricerri, M. A., and Jonas, A. (2004) Enthalpy-driven apolipoprotein A-I and lipid bilayer interaction indicating protein penetration upon lipid binding, *Biochemistry 43*, 12258−12264.
26. Pownall, H., Pao, Q., Hickson, D., Sparrow, J. T., Kusserow, S. K., and Massey, J. B. (1981) Kinetics and mechanism of association of human plasma apolipoproteins with dimyristoylphosphatidylcholine: Effect of protein structure and lipid clusters on reaction rates, *Biochemistry 20*, 6630−6635.
27. Swaney, J. B. (1980) Properties of lipid apolipoprotein association products: Complexes of dimyristoyl phosphatidylcholine and human apo A-I, *J. Biol. Chem. 255*, 877−881.
28. Kyte, J., and Doolittle, R. F. (1982) A simple method for displaying the hydropathic character of a protein, *J. Mol. Biol. 157*, 105−132.
29. Monera, O. D., Kay, C. M., and Hodges, R. S. (1994) Protein denaturation with guanidine hydrochloride or urea provides a different estimate of stability depending on the contributions of electrostatic interactions, *Protein Sci. 3*, 1984−1991.

BI702332B